Multiple-wavelength plasmonic nanoantennas

Svetlana V. Boriskina* and Luca Dal Negro

Department of Electrical and Computer Engineering and Photonics Center, Boston University, Boston, Massachusetts 02215, USA
**Corresponding author: sboriskina@gmail.com*

Received November 2, 2009; revised December 21, 2009; accepted January 7, 2010; posted January 11, 2010 (Doc. ID 119377); published February 11, 2010

We propose a type of photonic-plasmonic antennas capable of focusing light into subwavelength focal point(s) at *several* wavelengths, which are formed by embedding conventional dimer gap or bow-tie nanoantennas into multiple-periodic gratings. Fano-type coupling between localized surface plasmon resonances of dimer antennas and photonic modes in the gratings adds new functionalities, including multiple-wavelength operation and controllable enhancement of the field intensity in the focal point. Multiple-wavelength operation of nanoantennas provides tremendous opportunities for broadband single-molecule fluorescence and Raman sensing, emission enhancement, and near-field imaging. © 2010 Optical Society of America

OCIS codes: 240.6680, 250.5403, 290.4020.

Nanoantennas that couple optical waves into localized surface plasmons show potential for optical manipulation [1], fluorescence enhancement [2], nonlinear spectroscopy [3], optical characterization, etc. [4,5]. Typical dimer antennas consist of two metal nanoparticles (spheres, rods, triangles, etc.) coupled through a nanometer-scale gap. They provide resonant enhancement of the electric field in a subwavelength focal point (dimer gap) if the wavelength of the incident field is matched to the antenna localized surface plasmon (LSP) wavelength. LSP resonances of nanoantennas can be tuned by the choice of material, by engineering the particles shapes [6], and by introducing nanoloads in the gap [7]. Nanoantennas spectra can also be tailored to provide a resonant peak at wavelength λ_r by embedding them into one-dimensional (1D) or two-dimensional (2D) periodic gratings with period $d \approx \lambda_r$ [8,9], owing to coupling of LSPs to the photonic modes in the gratings. In this Letter, we propose a design strategy to obtain multifrequency field enhancement in the subwavelength focal spot(s) of dimer antennas by engineering coupling of antenna LSPs to photonic modes of multiple-periodic gratings. Antennas composed of spherical Ag nanoparticles are designed by using generalized Mie theory [10]; however, the design strategy and conclusions are general and do not depend on the specific choice of particles shapes and materials.

A multiple-wavelength multifocal nanoantenna is shown in Fig. 1(a) and consists of three identical nanoparticle dimers, each embedded into a 1D double-arm periodic grating of 10 periods in length and a different periodicity in the y direction. Hereafter, the dimers are composed of 50-nm-radius spheres coupled via a 20-nm-wide gap, which is achievable by using standard e-beam lithography [3,11]. The separation between the antennas in the x direction is large enough (1 μm) to avoid their cross talk. The plots of intensity enhancement in three focal points under illumination by a plane wave are shown in Fig. 1(b) and feature peaks at the wavelengths determined by the gratings periodicities. These peaks are a result of the Fano-type coupling between the grating narrow-linewidth photonic resonance (discrete energy level) and the broad LSP resonance of the dimer nanoantenna (continuum). The antenna near-field patterns calculated at the peak wavelengths [Figs. 1(c)–1(e)] demonstrate formation of photonic-plasmonic modes in each 1D grating. All the designs discussed here are optimized for normal illumination by a plane wave linearly polarized along the dimer axis, since it produces more than 1 order-of-magnitude intensity enhancement over illumination with the light of opposite polarization [3]. Diffractive

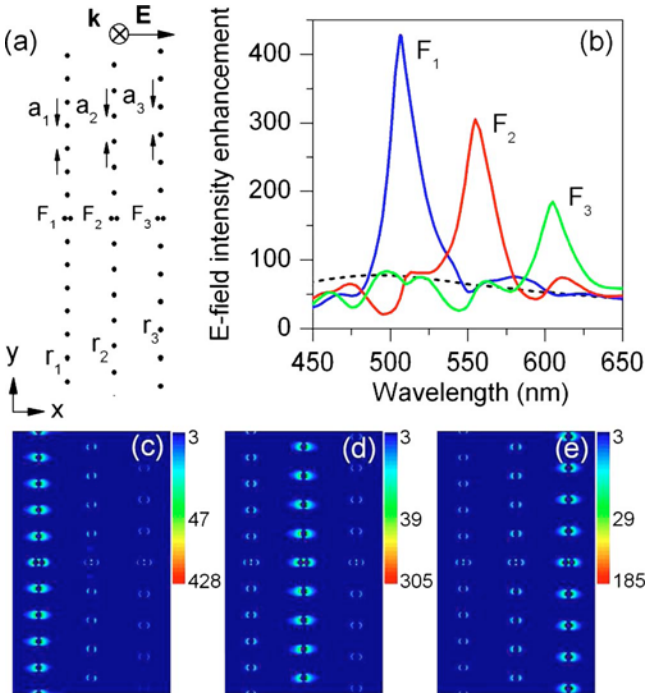

Fig. 1. (Color online) Multifocal photonic-plasmonic antenna. (a) Schematic of a multifocal antenna. (b) Intensity enhancement in three antenna foci as a function of the wavelength of the incident field for r_1=55 nm, a_1=500 nm, r_2=60 nm, a_2=550 nm, r_3=65 nm, and a_3=600 nm. Intensity enhancement in a dimer is shown as a dashed line. (c)–(e) Near-field intensity distributions (log scale) in the central part of the antenna at three wavelengths (λ_1 =507 nm, λ_1=557 nm, and λ_2=610 nm) corresponding to the peaks in Fig. 1(b).

0146-9592/10/040538-3/$15.00

coupling between nanoparticles in linear gratings is also maximized if both polarization and wave vector of the incident plane wave are perpendicular to the grating axis (as metal particles act as dipoles emitting in the directions perpendicular to their dipole moments, and their constructive interference is maximized if they all oscillate in phase) [9].

To formulate the design rules for achieving optimal field enhancement at a chosen frequency, we first studied the effect of the grating length on the focal point intensity. It can be seen in Fig. 2(a) that by increasing the number of grating periods the intensity can be boosted, however, at the expense on the larger device footprint. Previous studies revealed saturation of the enhancement growth at the chain length of ~400 periods [8]. We also explored other configurations of periodic gratings, including a four-arm grating, with the particle chains shifted laterally from the dimer position by half the grating period, and a six-arm grating [see insets in Fig. 2(b)]. Figure 2(b) demonstrates that the lateral expansion of the grating can also increase the focal point intensity. The peak wavelengths blueshift with the increase of the grating length, and saturate at the values close to the grating period [see Fig. 2(c)], which reflects formation and narrowing of the Fano-type resonant feature as a result of the decrease of the linewidth of the photonic resonance in longer gratings [see Fig. 2(a)]. Finally, the focusing efficiency of the grating can be improved by tuning the size of the particles [see Fig. 2(d)]. The increase in the particle sizes also redshifts the resonant peak; therefore, in order to tune the antenna to a specific wavelength, both grating period and particle radii should be adjusted simultaneously.

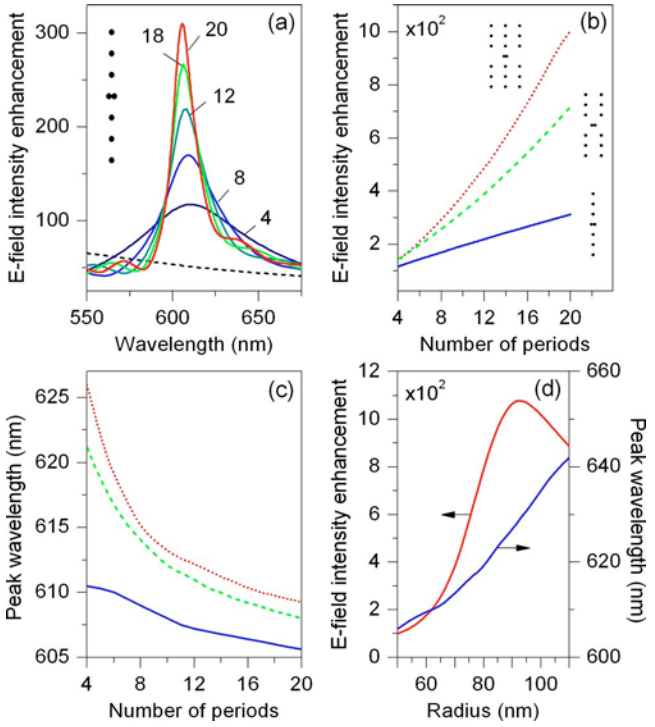

Fig. 2. (Color online) Role of grating length and configuration. (a) Intensity enhancement in the gap of a dimer embedded in a 1D two-arm grating with $r=70$ nm, $a=600$ nm (see inset) as a function of the wavelength and the grating length. The labels indicate the number of periods in each grating arm, and the dashed line shows the intensity in the bare dimer. Scaling of the focal spot intensity (b) and the peak wavelength (c) with the number of grating periods for the three gratings shown in the insets of Fig. 2(b). (d) Focal point intensity scaling and peak intensity wavelength shift in the antenna with the ten-period six-arm grating [dotted lines in (b) and (c)] with the change of the radii of the particles in the grating.

Next we investigate light focusing into a *single* subwavelength spot at *multiple* frequencies, which can provide a remarkable range of new functionalities to optical nanoantennas, including resonant enhancement of both pumping and emission efficiency of emitters, background free sensing of optically trapped nano-objects, broadband near-field imaging, etc. We design single-focal multiwavelength antennas by arranging gratings of different periodicities and configurations around a single focal point (dimer) as shown in Fig. 3(a). Three grating periods were chosen within the visible part of the spectrum (420, 500, and 600 nm), and the grating arms are 10 periods in length. Simulations of the multiple-periodic-grating antenna reveal well-defined resonant peaks in its extinction efficiency [Fig. 3(b)] and near-field intensity [Fig. 3(c)] spectra at the wavelengths corresponding to the grating periods. An additional peak at 388 nm reflects the situation when two wavelengths fit into the largest grating period. The extinction efficiency is calculated as the ratio of the extinction cross-section C_{ext} (a sum of the scattering and absorption cross-sections [10]) to the antenna metal volume: $Q_{\text{ext}}=C_{\text{ext}}/\pi a_c^2$, where $a_c=(3V_c/4\pi)^{1/3}$, and V_c is the combined volume of all the particles. The radii of the particles in the gratings of different periodicities were

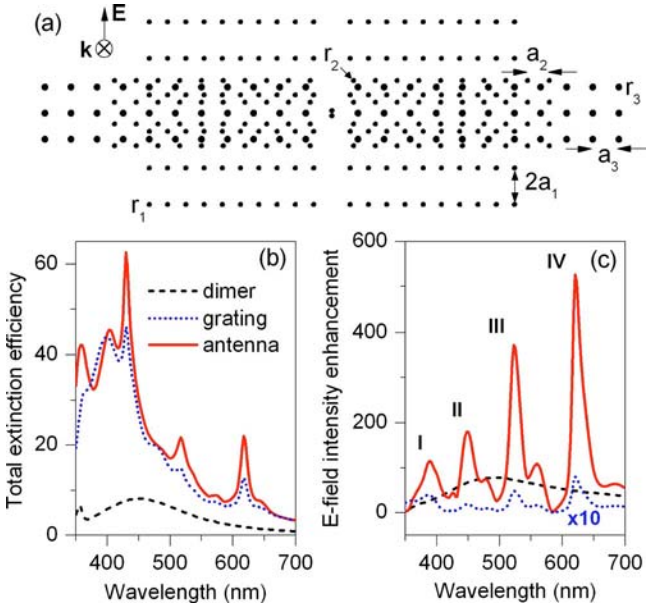

Fig. 3. (Color online) Multiple-wavelength photonic-plasmonic antenna. (a) Schematic of the multiple-wavelength antenna ($r_1=50$ nm, $a_1=420$ nm, $r_2=55$ nm, $a_2=500$ nm, $r_3=70$ nm, and $a_3=600$ nm). Total extinction efficiency (b) and focal point intensity enhancement (c) in the dimer (dashed), multiple-periodic grating without a dimer (dotted) and grating-assisted antenna (solid) as a function of wavelength.

tuned to optimize for the highest intensity enhancement; however, intersecting three gratings around a single focal point imposes geometrical constrains on the maximum size of the particles to avoid their overlaps and strong quasi-static coupling between different gratings at distances less than 25 nm. Therefore, in the practical design of multiple-grating antennas, one should look for an optimal trade-off between achieving maximum intensity and fitting geometrical constrains. The intensity distributions in the multiple-wavelength antenna at the resonant peaks are visualized in Figs. 4(a)–4(d) and demonstrate formation of photonic-plasmonic modes in different parts of the multiple-periodic grating.

Finally, we investigate the effect of the spectral mismatch of the dimer LSP resonance and the grating photonic-plasmonic resonance. The spectral position of the dimer LSP resonance can be tuned across the visible band by changing the radii of the nanoparticles comprising the dimer [see Fig. 5(a)]. In Fig. 5(b), we plot the focal point intensity in the six-arm-grating nanoantenna considered in Fig. 2(d) and observe the highest near-field enhancement when the LSP resonance and the grating modes are optimally spectrally tuned.

Based on the observed effects, we formulated the design rules for tailoring the resonant spectra of the multiple-wavelength antennas. First, by choosing the geometry and material of the dimer, its spectrum can be shaped to feature one or more peaks of high near-field intensity in the frequency range of interest [6]. Then, a multiple-periodic grating can be configured to enhance the focal spot intensity at selected wavelengths. This can be done by setting the period of each grating to the chosen wavelength value, and tuning the particle sizes to spectrally overlap the particle LSP resonance with the grating mode. Finally,

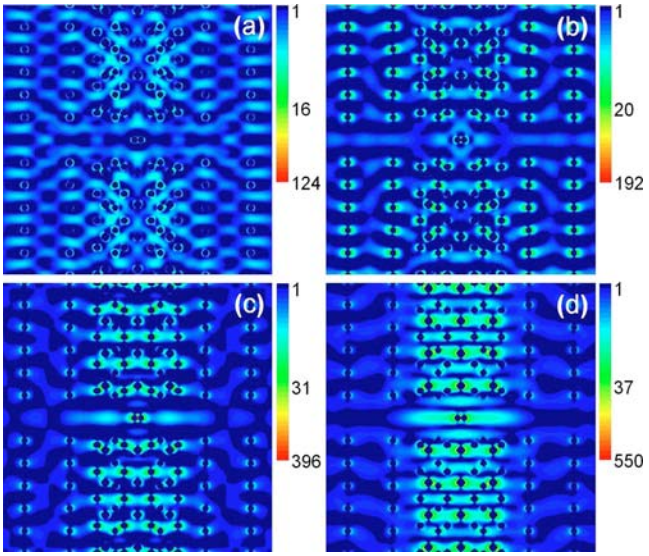

Fig. 4. (Color online) Near-field intensity distributions (log scale) in the multiple-wavelength antenna at the wavelengths (λ_1=388 nm, λ_2=449 nm, λ_3=523 nm, and λ_4=621 nm) corresponding to the four peaks in Fig. 3(c). At each wavelength, a high-intensity hot spot is created in the dimer gap.

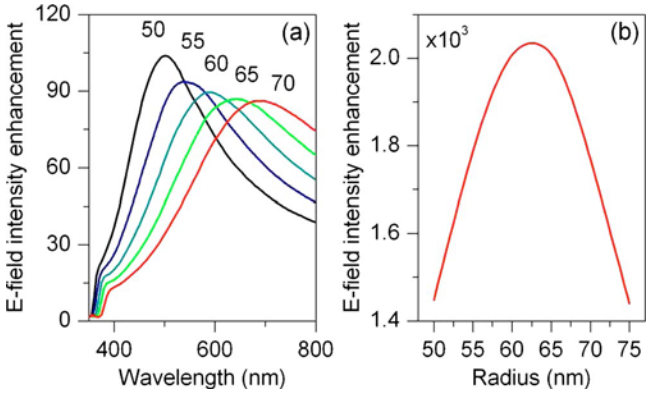

Fig. 5. (Color online) Optimization of the dimer-grating coupling efficiency. (a) Focal point intensity in a bare dimer (gap 15 nm) as a function of wavelength and the radii of the nanoparticles (labeled in the units of nm). (b) Scaling of the focal point intensity in the optimized (r=95 nm) 20-period six-arm single-wavelength antenna [same as in Fig. 2(d)] with the radii of the particles in the dimer.

the design can be fine tuned to make trade-offs between optimal particle sizes and geometrical constrains on nesting multiple gratings and between the antenna total length and maximum enhancement. Note that the reported intensity enhancement for the nanosphere dimer is the lowest estimate of the achievable enhancement if the particles with sharp edges are used [2,3,11].

Summarizing, we demonstrated grating-assisted nanoantennas that provide *multiwavelength* focusing in a *single* subwavelength spot, which paves the way for their application for multispectral single-molecule linear and nonlinear spectroscopy. The proposed antennas can also be integrated on a facet of an optical fiber or a laser [5] to be used as tools for optical data storage, near-field imaging, and optical lithography.

We thank Prof. Federico Capasso and his group members for stimulating discussions.

References

1. A. N. Grigorenko, N. W. Roberts, M. R. Dickinson, and Y. Zhang, Nat. Photonics **2**, 365 (2008).
2. R. M. Bakker, H.-K. Yuan, Z. Liu, V. P. Drachev, A. V. Kildishev, V. M. Shalaev, R. H. Pedersen, S. Gresillon, and A. Boltasseva, Appl. Phys. Lett. **92**, 043101 (2008).
3. P. J. Schuck, D. P. Fromm, A. Sundaramurthy, G. S. Kino, and W. E. Moerner, Phys. Rev. Lett. **94**, 017402 (2005).
4. P. Bharadwaj, B. Deutsch, and L. Novotny, Adv. Opt. Photon. **1**, 438 (2009).
5. E. Cubukcu, E. A. Kort, K. B. Crozier, and F. Capasso, Appl. Phys. Lett. **89**, 093120 (2006).
6. H. Fischer and O. J. F. Martin, Opt. Express **16**, 9144 (2008).
7. A. Alù and N. Engheta, Nat. Photonics **2**, 307 (2008).
8. S. Zou, N. Janel, and G. C. Schatz, J. Chem. Phys. **120**, 10871 (2004).
9. S. Zou and G. C. Schatz, J. Chem. Phys. **121**, 12606 (2004).
10. Y.-L. Xu, Appl. Opt. **34**, 4573 (1995).
11. A. Gopinath, S. V. Boriskina, B. M. Reinhard, and L. Dal Negro, Opt. Express **17**, 3741 (2009).